Small-angle Krein collisions in a family of four-dimensional reversible maps

A. Bhowal and T. K. Roy
Saha Institute of Nuclear Physics, 1/AF Bidhan Nagar, Calcutta 700 064, India

A. Lahiri
Vidyasagar Evening College, Calcutta 700 006, India

(Received 15 June 1992)

The small-angle Krein collision (SAKC) in four-dimensional reversible maps refers to the codimension-2 bifurcation, where the eigenvalues of the Jacobian of the map at a symmetric fixed point collide close to $+1$ as some relevant parameters are varied. SAKC is always associated with the bifurcation of nearby fixed points. We investigate the existence and stability of invariant curves around these fixed points for a particular family of reversible maps, and find a rich structure of the phase space.

PACS number(s): 05.45.+b, 03.20.+i

I. INTRODUCTION

In four-dimensional (4D) reversible maps, one of the various possible bifurcations at a symmetric fixed point is the so-called reversible Hopf bifurcation [1], in which two pairs of multipliers (eigenvalues of the Jacobian matrix) on the unit circle undergo a Krein collision [2] and move off along a pair of conjugate rays making angles $\pm\phi_0$ (say) with the positive real axis as a control parameter (say, ϵ) is varied. This situation was studied in Ref. [1], when the collision angle ϕ_0 was subjected to a set of nonresonance conditions that included, in particular, $\phi_0 \neq 0$, although it is quite possible that such instabilities can also occur when the multipliers move off very close to (1,0). In this case, not studied before, we find several new features, corresponding to what may be termed a "small-angle Krein collision" (SAKC). SAKC can occur in various contexts pertaining to reversible maps. In SAKC, the presence of two or more nearby fixed points, depending on the symmetry of the map, gives rise to a rich structure of the phase space close to the bifurcation.

In this paper we study the bifurcation of invariant curves (IC's, see below) around the fixed points for a particular two-parameter family of maps undergoing SAKC (Sec. II). Section III deals with their linear stability, suggesting a representative local structure of the overall phase space. Illustrations with numerical support are given in Sec. IV. Section V is devoted to concluding remarks.

II. BIFURCATION OF INVARIANT CURVES AROUND FIXED POINTS IN SAKC

A map A is said to be reversible [3] if there exists an involution G ($G\cdot G=I$) which reverses the action of A, i.e.,

$$G\cdot A\cdot G = A^{-1} ,$$

so that AG and GA are also involutions. In other words, a reversible map can be expressed as a product of two involutions,

$$A = AG\cdot G = G\cdot GA .$$

A well-known example is the $2m$-dimensional volume-preserving De Vogelaere map [4,5], which can be expressed as a second-order difference equation of the form

$$R_{n+1}-2R_n+R_{n-1}=F(R_n) , \tag{1}$$

where R_n is an m-dimensional vector and F is a vector-valued function.

We define an invariant set Γ of A as that which is mapped onto itself by the action of A: $A\Gamma=\Gamma$. Examples of invariant sets are fixed points, periodic orbits, invariant curves, invariant tori, etc. Invariant sets that are also invariant with respect to the reversing involution G (and therefore belonging to the symmetry set given by fixed points of G) are called symmetric invariant sets. For a symmetric fixed point, the multipliers, which are the eigenvalues of the Jacobian at that point, always occur in reciprocal pairs [6] (λ_1, λ_1^{-1}, λ_2, λ_2^{-1}, etc.). In the vicinity of symmetric fixed points, a reversible map behaves locally like a symplectic one [7–9]. We describe SAKC at these symmetric fixed points.

Consider the two-parameter family of 4D De Vogelaere maps given by Eq. (1) with a particularly simple form of F such that Eq. (1) reduces to a pair of coupled 2D maps,

$$A_G:\ \begin{cases} x_{n+1}-2x_n+x_{n-1}=px_n+y_n , \\ y_{n+1}-2y_n+y_{n-1}=-\epsilon x_n+py_n+g(x_n) , \end{cases} \tag{2}$$

with the linear part described by parameters ϵ,p, both of which will be taken to be sufficiently small so as to give rise to multipliers at the origin close to $+1$. The nonlinear part is so chosen that A_ϵ can be expressed as a single fourth-order difference equation,

$$x_{n+2}+x_{n-2}-2(p+2)(x_{n+1}+x_{n-1}) +[(p+2)^2+2+\epsilon]x_n=g(x_n) . \tag{3}$$

The form of the nonlinear function $g(x_n)$ will be described below. First consider the case $p<0$. For

$-p^2<\epsilon<0$, both pairs of multipliers at the origin O ($x_n=0$, $y_n=0$: a symmetric fixed point) lie on the unit circle. Outside this range of ϵ the multipliers do not all lie on the unit circle, with either a pair on the real axis (when $\epsilon<-p^2$, the other pair being on the unit circle) or both outside the unit circle [see Figs. 1(a)–1(e)]. The Krein collision occurs at angle $\phi_0=\cos^{-1}(1+p/2)$. The multipliers in the former case (i.e., for one of the pairs on the unit circle) correspond to a 2D local stable manifold coexisting with a 2D unstable one (described by the other pair on the real axis). We shall refer to this as "cylindrical instability" because the orbits starting near O in such cases appear to lie on the surface of a cylinder when two dimensional projections are plotted (see Sec. IV). The problem can also be addressed when $p>0$ (p small), for which the dispositions of the multipliers are given in Figs. 2(a)–2(e). Here the multipliers are all on the real line for $-p^2<\epsilon<0$. For $\epsilon<-p^2$, one of the pairs enters the unit circle and for $\epsilon>0$, both pairs move off the real line.

The map A_ϵ is reversible with respect to the involution G:

$$R'=S,\quad S'=R\ ,$$

where

$$R=\begin{bmatrix}x_n\\ y_n\end{bmatrix}\quad\text{and}\quad S=\begin{bmatrix}x_n-x_{n-1}\\ y_n-y_{n-1}\end{bmatrix}$$

are two-dimensional vectors. The origin O is a symmetric fixed point of A_ϵ. It is to be noted that the other fixed points near the origin given by real solutions to $(p^2+\epsilon)\bar{x}=g(\bar{x})$ are also symmetric. A discussion on the fixed points and their bifurcations follows later in this section.

As shown earlier in the case of the large-angle Krein collision (LAKC) [1,2], the bifurcation in question is sufficiently described by terms up to degree 3, so that we can take $g(x_n)=\alpha x_n^2+\beta x_n^3$. Depending on a parameter $\gamma=\gamma(\alpha,\beta)$ of the problem, two types of bifurcations were observed, normal (for $\gamma>0$) and inverted ($\gamma<0$) [1,2]. In the former case, two families of stable IC's exist arbitrarily close to the origin O for $\epsilon<0$, merge at $\epsilon=0$, and then move away from the origin as ϵ becomes positive. In the inverted bifurcation, families of IC's, elliptic and hyperbolic, shrink to the fixed point as $\epsilon\to 0$ from below and there occur no invariant curves for $\epsilon>0$.

For p small, all the above features are observed in SAKC as well, with some additional modifications of the phase-space structure due to the presence of at least one

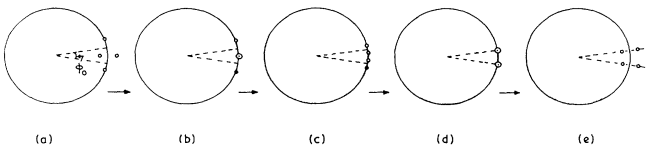

FIG. 1. Dispositions of the multipliers at origin for $p<0$ corresponding to (a) $\epsilon<-p^2$, (b) $\epsilon=-p^2$, (c) $\epsilon>-p^2$, (d) $\epsilon=0$, and (e) $\epsilon>0$.

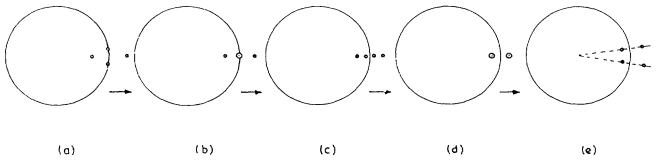

FIG. 2. Same as in Fig. 1 but for $p>0$.

symmetric fixed point near O. To describe the picture around O, we start with the fourth-order difference equation (3). As before we find that, although the number of fixed points depends on $g(x_n)$, the nature of the phase space around these fixed points depends on terms up to cubic order; we take $g(x_n)=\alpha x_n^2+\beta x_n^3$, where we choose $|\beta|=1$ through an appropriate scaling.

We investigate the phase-space structure around $\epsilon=0$, $p=0$, concentrating on the fixed points and IC's. The fixed points besides O are given by $x_n=\bar{x}$ (all n) with

$$\bar{x}=\{\alpha\pm[\alpha^2+4\beta(p^2+\epsilon)]^{1/2}\}2\beta\ . \tag{4}$$

The IC's will be obtained below in an order-by-order perturbation scheme for parameter values close to the SAKC. An IC with rotation number $\phi/2\pi$ may be represented by the Fourier series

$$x_n=\{a+b\exp(in\phi)+c\exp(2in\phi)+\ldots\}+\text{c.c.}\ , \tag{5}$$

where the coefficients $a,b,c,\ldots$ are expected to decrease with increasing n. Expressing the coefficients as $a=\sum_k a_k$, $b=\sum_k b_k$, etc. (with $a_k,b_k,\ldots$ depending on ϵ,p,ϕ and k denoting the order of smallness) perturbation expansion yields, for leading contributions, to the series

$$a_0=\frac{2\alpha b_0^2}{p^2+\epsilon}\ , \tag{6a}$$

$$b_0^2=\frac{\epsilon+[p+4\sin^2(\phi/2)]^2}{\gamma}\ , \tag{6b}$$

and

$$c_0=\frac{\alpha b_0^2}{\epsilon+[p+4\sin^2\phi]^2}\ , \tag{6c}$$

where

$$\gamma=3\beta+2\alpha^2\left[\frac{2}{p^2+\epsilon}+\frac{1}{\epsilon+(p+4\sin^2\phi)^2}\right]\ .$$

The bifurcation picture depends on the signature of γ and can be obtained from the requirement of a positive b_0^2. For $\gamma>0$, we have a "normal" bifurcation and for $\gamma<0$ an "inverted" bifurcation (described below). The higher-order terms $O(b_0^3)$ that will be required to test the accuracy of the estimated curves (see Sec. IV) are given by

$$d_0=\frac{b_0^3\left[\beta+\dfrac{2\alpha^2}{\epsilon+(p+4\sin^2\phi)^2}\right]}{\epsilon+[p+4\sin^2(3\phi/2)^2]^2}\ , \tag{6d}$$

$$e_0=\frac{3\beta b_0^2c_0+2\alpha b_0d_0+\alpha c_0^2}{\epsilon+(p+4\sin^2\phi)^2}\ , \tag{6e}$$

$$a_1=\frac{1}{p^2+\epsilon}[4\alpha b_0b_1+\alpha(a_0^2+2c_0^2)+3\beta(c_0+2a_0)b_0^2]\ , \tag{6f}$$

$$b_1=\frac{2\alpha c_0d_0+\beta(3b_0^2d_0+3a_0^2b_0+6c_0^2b_0+6a_0b_0c_0)}{q}+\frac{2\alpha b_0}{q}\left[\frac{\alpha(a_0+2c_0^2)+3\beta(c_0+2a_0)b_0^2}{p^2+\epsilon}+\frac{2\alpha(a_0c_0+b_0d_0)+3\beta(2c_0+a_0)b_0^2}{\epsilon+(p+4\sin^2\phi)^2}\right]\ , \tag{6g}$$

$$c_1=\frac{1}{\epsilon+(p+4\sin^2\phi)^2}\left[2\alpha b_0b_1+2\alpha(b_0d_0+a_0c_0)+3\beta b_0^2(a_0+2c_0)\right]\ , \tag{6h}$$

where

$$q=\epsilon+[p+4\sin^2(\phi/2)]^2-[9\beta b_0^2+6\alpha(a_0+c_0)]\ .$$

With $\phi/2\pi$ irrational [so that the problem of zero denominators in the expressions (6a)–(6h) for the coefficients of the series (5) does not arise] these coefficients diminish for $b_0^2<p^2$, the rate of convergence of the series (5) increasing with the smallness of b_0^2. For $|\alpha|\sim 1$ and $\epsilon>-p^2$, γ is always positive (due to the small denominator in the second term in the expression of γ) so that there is only normal bifurcation. The two families of IC's for $-p^2<\epsilon<0$ exist for $\phi^2>\phi_2^2$ and $\phi^2<\phi_1^2$, where ϕ_1^2 and ϕ_2^2 ($>\phi_1^2$) are solutions to

$$|\epsilon|=4(\phi^2+p)^2\ . \tag{7}$$

These merge at $\epsilon=0$ into a single family which then recedes away from O. A special case of bifurcation occurs as ϵ crosses $-p^2$ from above. Here γ becomes negative and the IC's exist in one family only for $\phi^2<\phi_2^2$.

For α small [$O(p)$], on the other hand, inverted bifurcation occurs. Here new features distinct from that of LAKC appear, which we describe below for $\alpha=0$ (so that $\gamma=3\beta$) and for both $p<0$ and $p>0$.

Case 1: $p<0$

(1) Normal bifurcation ($\gamma>0$): For $\epsilon<-p^2$, all the IC's (existing in one family for $\phi^2>\phi_2^2$) are cylindrically unstable. As we shall see in a later section, from the two-dimensional projections of the IC's, the orbits appear to lie on the surface of a cylinder so that locally they are stable in one plane but unstable in the other. For $-p^2<\epsilon<0$, the IC's close to the origin are stable. There is a transition region where the orbits become cylindrically unstable. The next section shows that this instability occurs when a pair of multipliers of the IC's (see below) leave the unit circle along the real axis [as in Fig. 1(a)]. For $\epsilon>0$, the two families merge and all the IC's move from the origin through a minimum distance $b_0|_{\min}=\sqrt{\epsilon/\gamma}$ and are stable.

(2) Inverted bifurcation ($\gamma<0$): For $-p^2<\epsilon<0$ the IC's exist for $\phi_1^2<\phi^2<\phi_2^2$ with $\phi_2^2-\phi_1^2$ decreasing with $|\epsilon|$ as $\epsilon\to 0$. That is, the IC's shrink to the origin at $\epsilon=0$, and for $\epsilon>0$ there are no IC's. As in LAKC [1,2,10], the phenomenon of intermittency is likely to occur in this case. Section IV shows an interesting feature observed for $\epsilon<-p^2$, namely, there are two transition regions so that there exists an annular region of stability. The IC's close to the origin are cylindrically unstable and those outside the annular region are also unstable (hyperbolic). The multipliers of the orbits are similar to the multipliers in Figs. 1(a)–1(e) as we move off from the origin.

Case 2: $p>0$

(1) $\gamma>0$. A family of cylindrically unstable IC's exists with $|\phi|>|\phi_c|$ for $\epsilon<-p^2$, the members of which pass arbitrarily close to O, and as $\epsilon>-p^2$, they recede away from the origin with the same nature. For $\epsilon>0$, these IC's do not exist [as evident from the failure of the convergence of the series (5)].

(2) $\gamma<0$. A family of IC's arbitrarily close to O and cylindrically unstable for $\epsilon<-p^2$ exists with a limit in phase space corresponding to $|\phi|<|\phi_c|$. These shrink to O as $\epsilon\to-p^2$ ultimately being annihilated at $\epsilon=-p^2$.

Next we study what happens to the phase space in the vicinity of the fixed points given by

$$\bar{x}=\pm[(p^2+\epsilon)/\beta]^{1/2}\quad(\alpha=0)\ . \tag{8}$$

For $\beta>0$ these fixed points do not exist when $\epsilon<-p^2$, and for $\beta<0$ they disappear when $\epsilon>-p^2$. The phase space around $\bar{x}$ is described by

$$x_{n+2}+x_{n-2}-2(p+2)(x_{n+1}+x_{n-1})+[(p+2)^2+2+\epsilon']x_n=a'x_n^2+\beta'x_n^3\ , \tag{9}$$

with $\beta'=\beta$, $\alpha'=3[\beta(p^2+\epsilon)]^{1/2}$, and $\epsilon'=-3p^2-2\epsilon$, so that the stability of the fixed points will be exactly identi-

TABLE I. Nature of fixed points (FP's) and invariant curves (IC's) around them for $p<0$ ($\alpha=0$).

		Nature and multipliers		Nature and multipliers	
β	ϵ	FP ($x=0$)	IC's around FP	FP's $[x=\pm(p^2+\epsilon)^{1/2}]$	IC's around FP's
$+1$	$\epsilon<-p^2$	unstable Fig. 1(a)	unstable Fig. 1(a)	FP's do not exist	
	$-p^2<\epsilon<0$	stable Fig. 1(c)	stable near FP Fig. 1(c) unstable away Fig. 1(a)	unstable Fig. 1(a)	unstable Fig. 1(a)
	$0<\epsilon\ll p^2$	unstable Fig. 1(e)	stable Fig. 1(c)	unstable Fig. 1(a)	unstable Fig. 1(a)
-1	$\epsilon<-\frac{3}{2}p^2$	unstable Fig. 1(a)	annular region of stability Fig. 1(a)$\rightarrow$1(c)$\rightarrow$1(e)	unstable Fig. 1(a)	unstable Fig. 1(a)
	$-\frac{3}{2}p^2<\epsilon<-p^2$	unstable Fig. 1(a)	annular region of stability	stable Fig. 1(c)	stable Fig. 1(c)
	$-p^2<\epsilon<0$	stable Fig. 1(c)	stable near FP Fig. 1(c) unstable away Fig. 1(e)	FP's do not exist	
	$0<\epsilon\ll p^2$	unstable Fig. 1(e)	IC's do not exist	FP's do not exist	

cal to those in Figs. 1(a)–1(d) with ϵ replaced by ϵ'. The IC's around the fixed point are determined as before but now the nature of bifurcation depends on the new γ value, which is

$$\gamma' \approx -15\beta \,, \tag{10}$$

which shows that if for O there is normal (inverted) bifurcation then for the fixed points the bifurcation will be inverted (normal). But, as we shall see in the next section, the stability characteristics are different in details. The overall structure of the phase space is schematically presented in Tables I and II, which show how the features are interrelated.

An important point to note is that in all the cases above there seems to be a limit in the extent of the IC's in the phase space given by $b_0^2<p^2$, beyond which they cease to exist due to the divergence of the series (5). Further, as also stated in Refs. [1,2] the convergence of the series is assumed for those ϕ's for which the problem of small denominators in the expression for terms higher in the series can be avoided. This requires ϕ not only to be

TABLE II. Nature of fixed points FP's and invariant curves (IC's) around them for $p>0$ ($\alpha=0$).

		Nature and multipliers			
β	ϵ	FP ($x=0$)	IC's around FP	FP's $[x=\pm(p^2+\epsilon)^{1/2}]$	IC's around FP's
$+1$	$\epsilon<-p^2$	unstable Fig. 1 (a)	unstable Fig. 1(a)	FP's do not exist	
	$-p^2<\epsilon<0$	unstable Fig. 1(c)	unstable Fig. 1(c)	unstable Fig. 1(a)	unstable Fig. 1(a)
	$0<\epsilon\ll p^2$	unstable Fig. 1(e)	IC does not exist	unstable Fig. 1(a)	unstable Fig. 1(a)
-1	$\epsilon<-p^2$	unstable Fig. 1(a)	unstable Fig. 1(a)	unstable Fig. 1(c)	unstable Fig. 1(c)
	$-p^2<\epsilon<0$	unstable Fig. 1(c)	IC does not exist	FP's do not exist	
	$0\epsilon\ll p^2$	unstable Fig. 1(e)	IC does not exist	FP's do not exist	

nonresonant, i.e., $\phi \neq 2\pi p/q$ (p,q are integers and prime to each other) but strongly irrational so that the coefficients of terms approach zero faster than the denominators. Even then the convergence of the estimated series for $n \to \infty$ remains a conjecture.

III. STABILITY OF IC's AROUND FIXED POINTS

The stability of an IC around O can be studied from the tangent map at the orbit ($x_n = \bar{x}_n$, say). Thus if $\xi_n = x_n - \bar{x}_n$, then (for $\alpha = 0$)

$$\xi_{n+2} - \xi_{n-2} + 2(p+2)(\xi_{n+1} - \xi_{n-1}) + [(p+2)^2 + 2 + \epsilon - 3\beta\bar{x}_n^2]\xi_n = 0 \ . \quad (11)$$

As in Ref. 10, ξ_n can be expressed as

$$\xi_n = \lambda^n[1 + Ae^{in\phi} + A'e^{-in\phi} + Be^{2in\phi} + B'e^{-2in\phi} + \cdots] + \text{c.c.} \ , \quad (12)$$

where the possible values of λ, the "quasimultipliers," determine the stability of the orbit. But since $\epsilon - 3\beta x_n^2$ is quasiperiodic due to irrational ϕ, $\lambda e^{iN\phi}$ (where N is an arbitrary integer) is also a solution for the quasimultiplier. A consequence of this is that for $\lambda = \exp(i\psi)$, with ψ real for elliptically stable orbits, the quasimultipliers fill up the entire unit circle indicating the stability of the IC's. For λ lying off the unit circle the quasimultipliers fill up two circles with reciprocal radii (in addition, a trivial set of quasimultipliers fill up the unit circle; see Ref. [10]). The cylindrical instability corresponds to a nontrivial set of quasimultipliers lying on the unit circle. We therefore define the multipliers of an IC as the quartet of quasimultipliers (containing two reciprocal pairs), from which the entire set of quasimultipliers can be obtained by irrational rotations $N\phi$. An IC will become unstable when these multipliers move off the unit circle corresponding to ψ changing from real to complex. For b_0 small compared to ϵ the solutions to ψ are expected to be very near to ϕ, the rotation angle for the IC.

Representing the IC about O by its leading-order terms, namely, $\bar{x}_n = 2b_0 \cos n\phi$ ($\alpha = 0$), we equate coefficients of $\lambda^n e^{-2in\phi}$, $\lambda^n e^{2in\phi}$, etc., and eliminate B, B', etc., to arrive at (for $\alpha = 0$, either odd or even harmonics are present)

$$\epsilon - 6\beta b_0^2 + 4(\cos\psi - 1 - p/2)^2 = (3\beta b_0^2)^2 (1/\{\epsilon - 6\beta b_0^2 + 4[\cos(\psi - 2\phi) - 1 - p/2]^2\} + 1/\{\epsilon - 6\beta b_0^2 + 4[\cos(\psi + 2\phi) - 1 - p/2]^2\}) \ . \quad (13)$$

Note that $\psi = \pm\phi$ is always a solution to (13) provided we neglect one of the terms on the right-hand side (rhs) with respect to the other. Thus for an IC there will always be a trivial set of quasimultipliers filling up the unit circle corresponding to deviations ξ_n lying on the IC itself.

For the transition to elliptic stability (cylindrical instability) from cylindrical instability (elliptic stability) when $\epsilon = -p^2 \pm \delta$ (δ small), $b_0^4 \ll \epsilon$, the rhs of (13) can be neglected with respect to the lhs. As a result, (13) is simplified to

$$\epsilon - 6\beta b_0^2 + 4(\cos\psi - 1 - p/2)^2 = 0 \ . \quad (14)$$

This leads to (p and ψ being small)

$$\psi^2 = -p \pm [\epsilon + 2(\phi^2 + p)^2]^{1/2} \ . \quad (15)$$

TABLE III. Observed values of ϕ^2 (for transition to cylindrical instability) and $\delta\phi$ (for transition to hyperbolic instability).

β	p^2 (units of 10^{-5})	ϵ (units of 10^{-5})	ϕ^2 (calc.) (units of 10^{-2})	ϕ^2 (obs.) (units of 10^{-2})	$\delta\phi$ (calc.) (units of 10^{-2})	$\delta\phi$ (obs.) (units of 10^{-2})
-1	2.2	-3.0	0.985	0.988	2.30	2.37
		-1.0			1.33	1.40
	3.55	-4.5	1.23	1.24	2.51	2.60
		-2.0			1.67	1.77
	6.00	-7.0	1.58	1.58	2.75	2.85
		-3.0			1.80	1.91
	10.9	-2.0	2.29	2.31	3.99	4.10
		-0.8			2.53	2.67
$+1$	2.23	-1.5	0.905	0.904		
	3.55	-2.5	1.15	1.15		
	6.00	-5.0	1.52	1.52		
	10.9	-5.0	1.94	1.95		

For this transition one of the pairs of multipliers either enter or leave the real line (the other being on the unit circle) corresponding to ψ^2 crossing zero. The transition occurs at ϕ given by

$$\phi^2 = -p \pm [(p^2-\epsilon)/2]^{1/2} . \tag{16}$$

One or both solutions may not exist either due to poor convergence (here $p^2+\epsilon$ is small) of the series (5) when ϕ is small or for ϕ real. The other transition, from elliptic stability to hyperbolic instability, especially for $\beta<0$ and $\epsilon<0$, has been studied before in connection with similar problems in LAKC [11]. This time $b_0^2 \sim O(\epsilon)$ so that the rhs of Eq. (13) cannot be neglected as in the previous case. But because it is expected that $\psi \approx \phi = \phi_0 + \delta\phi$ the second term in the square brackets of the rhs can be neglected with respect to the first and a solution (with $\delta\phi \ll \phi_0$) to (13) is given by

$$\psi = \pm\{\phi \pm [2(\epsilon + 12\sin^2\phi_0 \delta\phi^2)]^{1/2} 2\sin\phi_0\} . \tag{17}$$

Therefore the multipliers of the IC are off the unit circle when

$$\delta\phi^2 < \delta\phi_c^2 = |\epsilon| / 12\sin^2\phi_0 . \tag{18}$$

The experimental values are expected to be a bit away from the estimate due to the approximation $\delta\phi \ll \phi_0$. This type of instability occurs only when $\beta<0$ and $p<0$.

The IC's around the other fixed points, however, have different stability characteristics. Since the condition $b_0^2 \ll |(p^2+\epsilon')| = |2(p^2+\epsilon_0)|$ is required for convergence, the stability of the IC's are dependent on $\epsilon' = -3p^2 - 2\epsilon$ alone, in the same way as that of the fixed point. To summarize, we list in Tables I and II the nature of the fixed points (including the origin O) and the stability of the IC's around these points exhibiting the bifurcation features as ϵ (and hence ϵ') is varied.

In the next section we illustrate through numerical result and graphical presentation the principal features of the bifurcations discussed above.

IV. NUMERICAL SUPPORT

All calculations were performed with double precision accuracy (to 14 significant digits) with the collision angle (for $p<0$) $\phi_0 \sim 10^{-2}$. Typically, most of the experiments were done with $\phi_0 = 2\pi/91.357\,973$ $[p = -\phi_0^2 = -(2.23 \times 10^{-5})^{1/2}]$ in order to approximate an irrational rotation. For positive p, we chose $\phi_0^2 = -p$ for comparison. To construct the IC's, initial values of x_j, $j = 1-4$, were chosen according to Eq. (5) and the map was iterated and then numerically tested against the perturbative solution. The iterates were found to lie on the estimated curve, the duration of which depended on the initial accuracy. As more terms in the series (5) were included, the number of iterates for persistence on the curve increased. A deviation or poor accuracy in the initial conditions resulted in the iterates ending up on a torus in the case of a stable curve, and escaping to infinity in the case of an unstable one.

Figures 3(a)–3(b) correspond to a two-dimensional projection of the curves on the plane $(x_n, u_n \equiv x_n - x_{n-1})$ for $\alpha=1$ and $\beta=1$ $[p = -(2.23\times10^{-5})^{1/2}]$. Normal bifurcation was observed for $\epsilon > -p^2$. The IC's initially close to O for $-p^2 < \epsilon < 0$ are pushed away from O as $\epsilon > 0$. There is a special bifurcation of the IC's to cylindrical instability when $\epsilon < -p^2$ [Fig. 3(c)].

The two types of bifurcation, normal and inverted, depending on the signature of γ, are observed when we

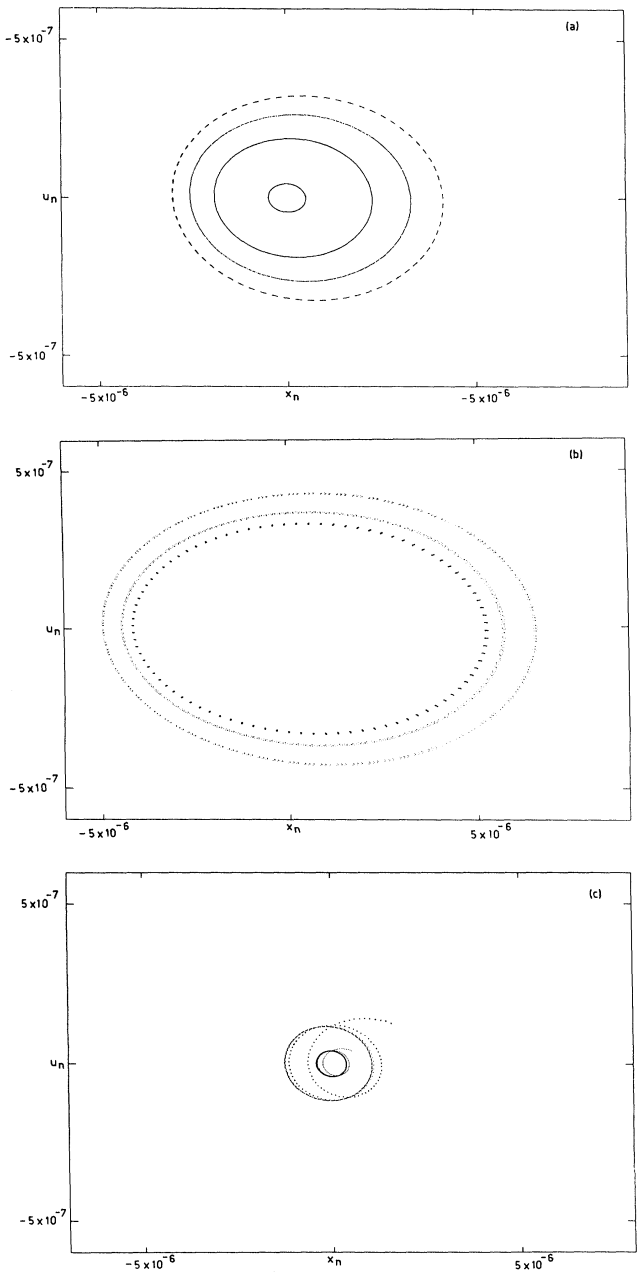

FIG. 3. Two-dimensional projection ($u_n \equiv x_n - x_{n-1}$ vs x_n) of IC's around origin for $\alpha=1$, $\beta=1$, $p=-(2.23\times10^{-5})^{1/2}$, $\phi_0 = 2\pi/91.357\,973$ for (a) $\epsilon = -2\times10^{-5}$ $(0>\epsilon>-p^2)$, (b) $\epsilon = 10^{-6}$ $(\epsilon>0)$, and (c) $\epsilon = -3\times10^{-5}$ $(\epsilon<-p^2)$. All figures are plotted in the same scale for comparison.

switch off α. Figures 4(a)–4(d) illustrate normal bifurcation for $\beta=1$, with ϵ increasing from $-p^2-\delta$ ($\delta>0$) to $\epsilon>0$. Initially, all the curves (for $\epsilon<-p^2$) are cylindrically unstable, a number of which become stable when ϵ crosses $-p^2$ from below. At this stage the transition values for which the curves become cylindrically unstable was also checked and found to agree well with that estimated by Eq. (16) (see Table III). The stability region increases as $\epsilon\to 0$. When ϵ crosses 0 from below, the IC's are repelled away from the origin.

Around the fixed points, the extent of the phase space accomodating the IC's being small, the stability, as we have seen in the preceding section, depends on the value of $\epsilon'=-3p^2-2\epsilon$. That is, as the curves around O become stable, those around the fixed points become cylindrically unstable (and vice versa).

The next set [Figs. 5(a)–5(c)] describe the interesting case for $\beta<0$ ($p<0$). For $\epsilon=-p^2-\delta$ ($\delta>0$), as expected, the curves close to O are cylindrically unstable, becoming stable for a larger value of b_0. For b_0 larger still, again the curves become unstable (hyperbolic), but this time they escape to infinity with rotation in both the planes. The transition values in both regions were tested and were found to agree well with the estimated values (Table III). For $\epsilon>0$ [Fig. 5(e)], the phenomenon of intermittency is found to occur as in Ref. [10].

Numerical experiments were performed with other values of $p<0$ (ϕ_0 real) as well as for both $\beta>0$ and $\beta<0$. The transitions to (from) elliptic stability from (to) cylindrical instability at the observed values for all of them were in excellent agreement with the theoretical values from Eq. (16) (Table III, columns 4 and 5). For the other transition, namely, from elliptic stability to hyperbolic instability, the observed values agreed with that of Eq. (18) to within 5% (Table III, columns 6 and 7).

The experiments with $p>0$ proved to be rather unsuccessful. The IC's in this case were difficult to construct, because of the high degree of cylindrical instability in most of the cases. The IC's were so unstable that even one full rotation of the points was hardly seen in any case. The best agreement is demonstrated in Fig. 6 for the case $\beta=1$, $\epsilon<-p^2$, for the IC's around O only, where it is seen how the degree of instability increases as we move away from the origin.

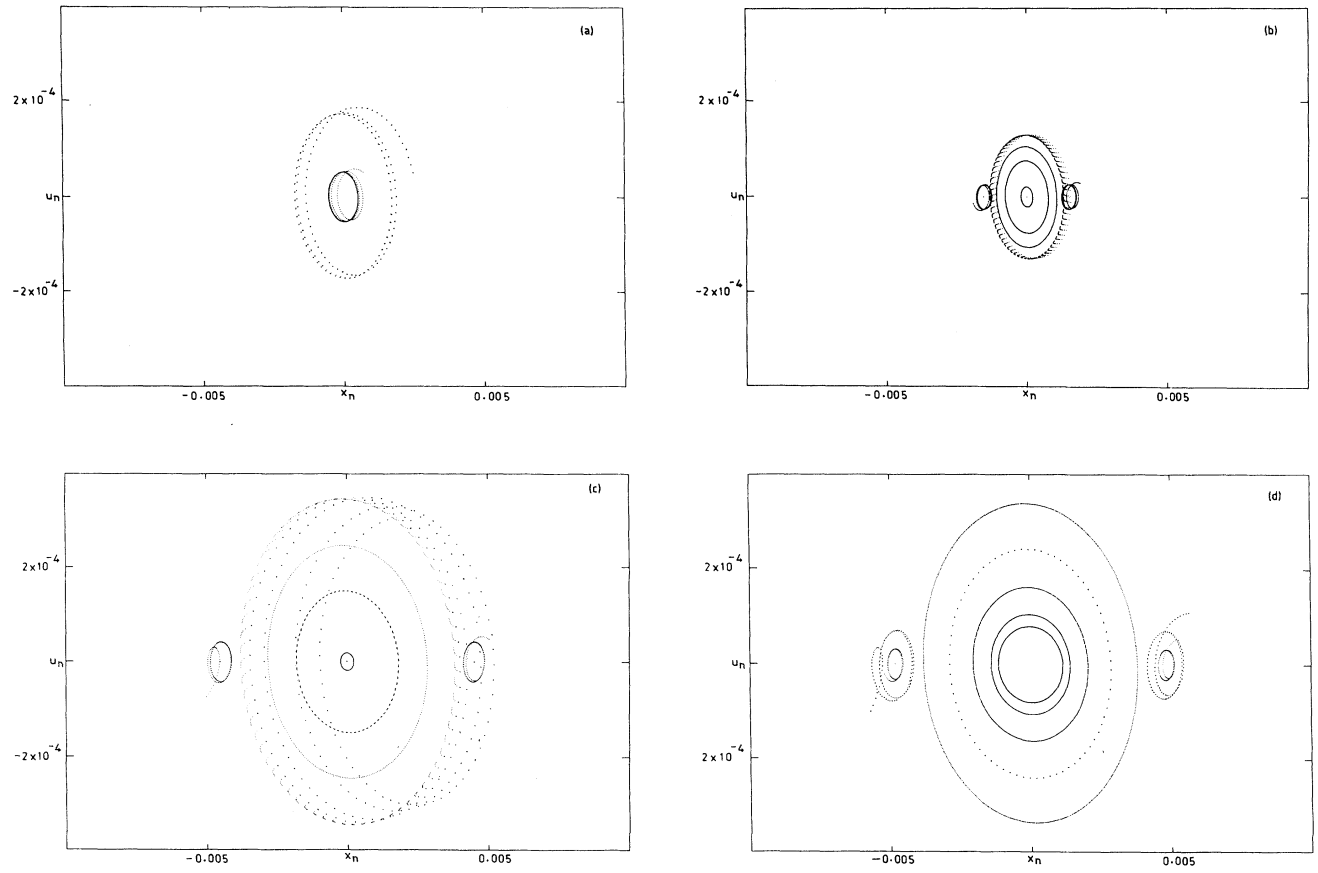

FIG. 4. Two-dimensional projection ($u_n\equiv x_n-x_{n-1}$ vs x_n) of IC's around origin and other two fixed points for $\alpha=0$, $\beta=1$, $p=-(2.23\times10^{-5})^{1/2}$, $\phi_0=2\pi/91.357\,973$ for (a) $\epsilon=-2.5\times10^{-5}$ ($\epsilon<-p^2$), (b) $\epsilon=-2\times10^{-5}$ ($0>\epsilon>-p^2$), (c) $\epsilon=-2\times10^{-6}$ ($0>\epsilon>-p^2$), and (d) $\epsilon=10^{-6}$ ($\epsilon>0$). All figures are plotted in the same scale for comparison. Notice how the stability region around the origin increases as $\epsilon\to 0$.

V. CONCLUSION

In this paper we have demonstrated the peculiarities of small-angle Krein collision (SAKC) [2] in a family of 4D reversible maps distinct from the features observed in the large-angle collision [1]. Since SAKC in reversible systems is always associated with the bifurcation of nearby fixed points, the regions of phase space around these fixed

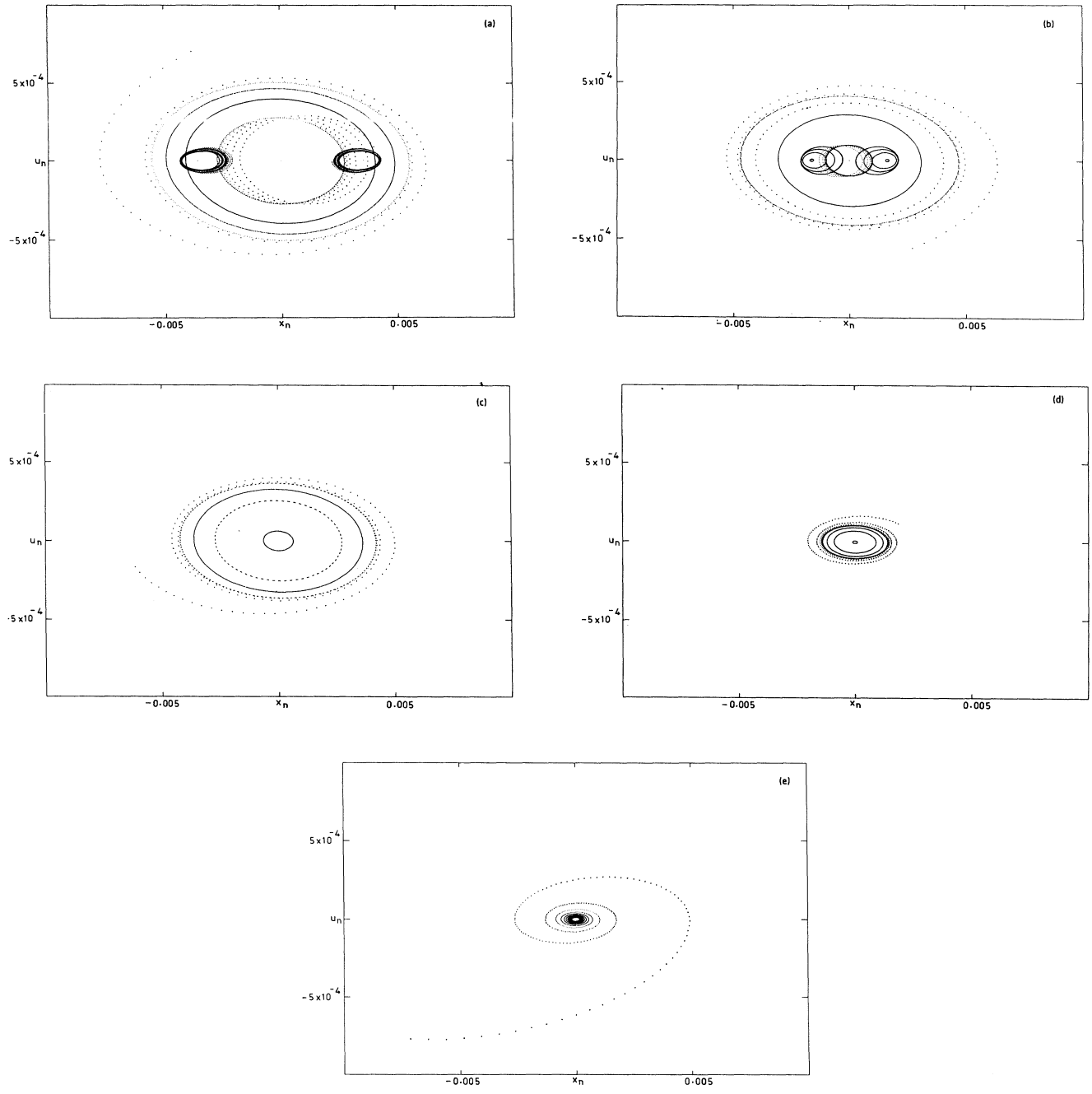

FIG. 5. Two-dimensional projection ($u_n \equiv x_n - x_{n-1}$ vs x_n) of IC's around origin and other two fixed points for $\alpha=0$, $\beta=-1$, $p=-(2.23\times10^{-5})^{1/2}$, $\phi_0=2\pi/91.357\,973$ for (a) $\epsilon=-3.5\times10^{-5}$ ($\epsilon<-\frac{3}{2}p^2$), (b) $\epsilon=-2.5\times10^{-5}$ ($\epsilon<-p^2$), (c) $\epsilon=-2\times10^{-5}$ ($0>\epsilon>-p^2$), (d) $\epsilon=-2\times10^{-6}$ ($0>\epsilon>-p^2$), and (e) $\epsilon=10^{-8}$ ($\epsilon>0$). All figures are plotted in the same scale for comparison. The cylindrical instability around the origin disappears for $\epsilon>-p^2$. The phase space accommodating the IC's shrinks as $\epsilon\to0$. Intermittency occurs for $\epsilon>0$ (initial conditions are taken at random).

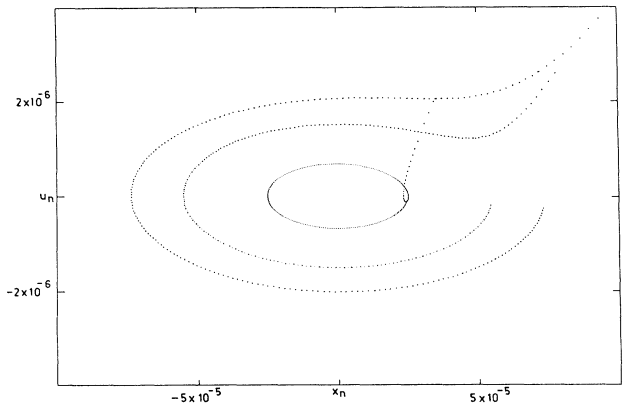

FIG. 6. Two-dimensional projection ($u_n \equiv x_n - x_{n-1}$ vs x_n) of IC's around origin for $p = +(2.23 \times 10^{-5})^{1/2}$, with other parameters same as in Fig. 4, for $\epsilon = -2.5 \times 10^{-5}$ ($\epsilon < -p^2$) only.

points are always correlated, leading to a rich variety of its structure. It is to be noted that because all the features in SAKC were observed around the symmetric fixed points, all of them can also be observed in symplectic maps as well.

We have discussed two classes of SAKC, corresponding to $p < 0$ and $p > 0$, a parameter characterizing the family of maps. While the former could be illustrated by numerical support and figures, the latter posed difficulties due to high degree of instabilities in the system.

We have considered SAKC for fixed points and IC's around them close to the bifurcation of the fixed points. This can also be applied in principle to describe invariant two-tori around bifurcating IC's in a reversible system with the points replaced by curves and curves by two-tori or, in general, to similar problems involving higher-dimensional tori. A simple variant is the case of invariant curves around bifurcating p-periodic orbits of a reversible map, where the angle of rotation per iteration is commensurate with 2π. The IC's around these orbits will be determined by a deviation $\delta\phi$ of the rotation angle from $2\pi/p$ with $\delta\phi$ an irrational multiple of 2π. For the orbits having multipliers near $+1$, these IC's will be described by SAKC. A future communication will illustrate an application to the case of invariant period-4 orbits bifurcating through collisions of multipliers at $\pm i$ on the unit circle. The latter has been studied recently in Ref. [12].

[1] M. B. Sevryuk and A. Lahiri, Phys. Lett. A **154**, 104 (1991); T. K. Roy and A. Lahiri, Phys. Rev. A **44**, 4937 (1991).

[2] The term "Krein collision" is used in this paper only because it has gained a certain amount of currency. A uniformly accepted nomenclature is yet to evolve in respect of the bifurcations studied here. The term "reversible Neimark-Sacker bifurcation" was used in Ref. [11], while in a few other works, it has been referred to as "reversible Hopf bifurcation."

[3] R. L. Devaney, Trans. Am. Math. Soc. **218**, 89 (1976).

[4] R. De Vogelaere, in *Contributions to the Theory of Nonlinear Oscillations,* edited by S. Lefschetz (Princeton University Press, Princeton, NJ, 1958), Vol. 4.

[5] J. M. Greene, R. S. Mackay, F. Vivaldi, and M. J. Feigenbaum, Physica D **3**, 468 (1981).

[6] *Reversible Systems,* edited by M. B. Sevryuk, Lecture Notes in Mathematics Vol. 1211 (Springer, Berlin, 1986).

[7] G. R. W. Quispel and J. A. G. Roberts, Phys. Lett. A **132**, 161 (1988).

[8] G. R. W. Quispel and J. A. G. Roberts, Phys. Lett. A **135**, 337 (1989).

[9] G. R. W. Quispel and H. W. Capel, Phys. Lett. A **142**, 112 (1989).

[10] A. Bhowal, T. K. Roy, and A. Lahiri (unpublished).

[11] A. Lahiri, A. Bhowal, T. K. Roy, and M. B. Sevryuk, Physica D **63**, 99 (1993).

[12] T. J. Bridges, J. Furter, and A. Lahiri, University of Utrecht Report No. NR739, 1992.